Relativistic electron enhancements, magnetic storms, and substorm activity

P. Bühler [a,1] L. Desorgher [b]

[a] *Paul Scherrer Institute, 5232 Villigen PSI, Switzerland*

[b] *University of Bern, 3012 Bern, Switzerland*

Abstract

The relativistic electron fluxes of the earth's outer radiation belt are subjected to strong temporal variations. The most prominent changes are initiated by fast solar wind streams impinging upon the magnetosphere, which often also cause enhanced substorm activity and magnetic storms. Using four years of data from the particle detector REM aboard the UK satellite Strv-1b in a GTO, we investigated the relation between these different appereances of geomagnetic activity. A typical sequence is that there is a drop in the relativistic electron intensity during the main phase of the magnetic storm and a successive enhancement during the recovery phase which sometimes leads to much higher than pre-storm fluxes. Whereas the flux drop is well correlated with the magnetic storm intensity and is mainly due to the deceleration and loss of particles caused by the ring-current induced magnetic field changes, there is only a bad correlation between the post-storm electron flux and Dst. As we show here, it is much more the level of substorm activity during the whole event which determines the size of the flux enhancements.

1 Introduction

The relativistic electron population trapped in the earth's outer radiation belt is known to be highly variable. Extensive theoretical and observational work has been carried out to identify various processes acting upon trapped particles to explain their dynamical behavior [1]. During geomagnetic quiet periods the changes of the trapped relativistic electron population are dominated by diffusion processes [2, 3], which are mainly responsible for the equilibrium structure of the radiation belts [4]. The involved time scales depend on energy and L-value. For few MeV electrons in the outer belt the rate of the apparent

[1] Corresponding author, E-mail address: paul.buehler@psi.ch

Preprint submitted to Elsevier Preprint *24 August 2000*

inward motion of the flux distribution is of the order of 0.03 R_E/day and the e-folding time of the loss processes is of the order of 10 days [5].

During geomagnetic active periods however much faster variations are observed, implying other processes to dominate [6]. The trigger for these changes are most often enhancements in the solar wind velocity and corresponding enhanced solar wind pressures upon the magnetosphere and/or changes of the Interplanetary magnetic Field, IMF. Most prominent are solar proton events, coronal mass ejections, CMEs, and corotating interaction regions, CIRs associated with high speed solar wind streams emerging from solar coronal holes.

The arrival of a solar wind disturbance at the earth typically causes first a rapid, less than a day, drop of the relativistic electron flux in the outer belt. In the following days, the flux can increase again and then turns over into a phase of slow decay [7, 1, 8].

Not all solar wind disturbances are equally efficient in producing high energy electrons. The maximum flux level reached after an event can be lower or higher than the flux before the event. The variations are linked with the properties of the solar wind stream impinging upon the magnetosphere and also of the IMF [9, 10]. It was noted that large electron fluxes are promoted by high solar wind speeds and southward IMF. The effectiveness of the solar wind - electron belt coupling shows a semiannual modulation with highest effectiveness around spring and fall and lower effectiveness during summer and winter [11, 12].

Solar wind disturbances are also the origin of substorm activity and magnetic storms. And although relativistic electron enhancements, magnetic storms and strong substorm activity occur typically simultaneously their relation is not clear. It has been noted that electron enhancements at Geostationary Orbit, GEO occur in association with magnetic storms [13] but the post-storm flux level does only poorly correlate with the size of the storm measured with Dst. During substorms energetic electrons can be injected into the trapping region and it has been proposed that these particles form a seed population which can be accelerated by a not yet defined process to higher energies which finally gives rise to the observed high energy electron enhancements [14].

With this paper we aim to clarify the role of storms and substorms in the production of relativistic electrons, and therefore investigate the relation between various solar wind parameters, geomagnetic indices and the solar wind disturbance induced relativistic electron variations.

2 Data and observations

As measure for the relativistic electron fluxes in the outer belt we use data from the particle detector Radiation Environment Monitor REM [15], which was operational from August 1994 to September 1998 aboard the UK satellite Strv-1b. Strv-1b was in a Geostationary Transfer Orbit, GTO with an inclination of 7° and a period of ≈ 10.5 hours. REM consists of two shielded silicon detectors. In this paper we use data from the detector covered with an aluminum cone of 0.81 g/cm^2 with a lower electron energy threshold of ≈ 1 MeV. We also use solar wind data from the Solar Wind Experiment [16] and IMF data from the Magnetic Fields Instrument [17] aboard the satellite Wind and geomagnetic indices from the National data centers, NOAA [18].

2.1 A typical event

Figure 1 shows various parameters during the period from 25 March to April 1 1995. The data presented here shows some typical features observed during the arrival of solar wind disturbances. The five uppermost panels show from top to bottom: solar wind velocity, solar wind dynamic pressure, IMF_{z}, Ap, and Dst. The sixth panel contains a quantity we denote as e_{cont} and is calculated with equation [1].

$$e_{cont} = \int_{4.0}^{6.8} L^2 \cdot cr \cdot dL \qquad (1)$$

where cr is the REM count rate. e_{cont} will be used here as a proxy for the number of relativistic electrons trapped in the outer belt. In the seventh panel the electron spectral index, γ_e measured with REM at $5.0 < L < 5.5$ $\mathrm{R_E}$ is plotted. To obtain this index, the differential electron energy spectra were approximated by an exponential function ($f_e(E) = f_0 \cdot E^{\gamma_e}$) and the free parameters f_0 and γ_e were obtained by a fitting procedure [15]. The lowest most row of panels show REM count rate L-profiles for selected belt passages in different colors. The periods of time covered by the profiles are marked with the corresponding colors in the Dst-panel.

The plotted example has typical features which are observed more or less pronounced in all the studied cases. The event is initiated by changes in the interplanetary conditions - an increase of solar wind velocity and dynamic pressure and enhanced variations of IMF_{z}. This causes enhanced substorm activity (high Ap-values) and also the development of a magnetic storm (decrease of Dst). During the main phase of the storm the relativistic electron fluxes decrease as shown in the left most count rate L-profile panel and the electron

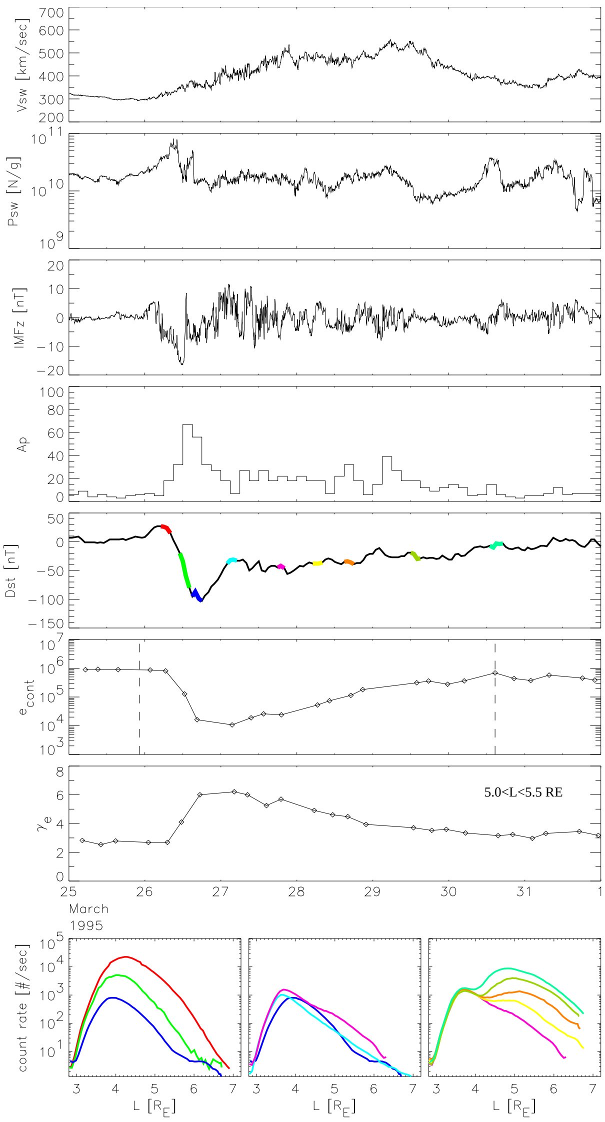

Fig. 1. A typical solar wind disturbance induced event. (t.t.b.) Solar wind velocity, solar wind dynamic pressure, IMF_z, Ap, Dst, electron exponential energy spectral index γ_e, and REM count rate profiles.

spectrum softens (increase of γ_e). Then during the following few hours little changes are observed (middle panel) until the count rates start to increase for the following days (right most panel). The increase is accompanied by a steady hardening of the electron spectrum.

2.2 *Flux dropouts*

The decrease of the electron flux during the main phase of the storm is mainly caused by the ring-current induced magnetic field decrease [19, 20, 21, 22]. The storm-time magnetic field changes are normally slow compared to the characteristic time scales associated with the adiabatic invariants of the trapped relativistic electrons such that the adiabatic invariants are in good approximation conserved. The decrease of the magnetic field therefore leads to a deceleration and outward movement of the electrons resulting in a drop of the electron flux at a given energy. Since the effect is most important at high energies the electron spectra are expected to soften, as is observed. The apparent inward drift of the flux distribution during the main phase (see left most count rate L-profile panel in figure 1) seems in a first view to be more difficult to explain with the Dst-effect because single particles tend to drift outward. However, due to the fact that energy loss and outward drift are more important at large L, the peak of the flux distribution moves inward [23].

The fact that post-storm fluxes are often lower than the pre-storm fluxes suggests that besides the adiabatic changes also real losses occur during the storm main phase. A potential candidate-process is loss of electrons from stable trapping due to the outward movement and interaction with the plasmapause [22]. Other processes are likely to be involved as well.

2.3 Flux enhancements

Whereas the observed electron flux dropouts are clearly linked with the storm main phase the occurrence of the flux enhancements is not as easily associated with a prominent feature, neither in solar wind, nor IMF, nor geomagnetic data. And although the occurrence of a fast solar wind stream producing a geomagnetic storm promises also to lead to a relativistic electron enhancement this is not always the case and visa-versa the absence of a large Dst-deviation does not guarantee low electron fluxes. So the question remains, what determines the post-event electron flux.

In order to address this question we selected a number of events between January 1995 and September 1998 and studied the correlation of the electron flux enhancements with different solar wind parameters and geomagnetic indices. We looked for periods during which at least one of the following criteria was fulfilled: V_{sw} raised above 500 km/sec, Dst went below -50 nT, Ap increased above 50 nT, or there were significant changes in the REM count rates. In addition the selection was restricted by the availability of solar wind and REM data. In 1998 REM was only sporadically operated, which limited the number of selected events for that year. The final list contains 58 events (31 in 1995, 12 in 1996, 12 in 1997, and 3 in 1998). For each of the events we defined a start and stop time, t_{start}, t_{stop}. The start was defined by the first appearance of significant changes in one of the solar wind parameters or geomagnetic indices and the stop time was defined by the time e_{cont} reached the maximum (see vertical dashed lines in the e_{cont}-panel of figure 1), with the restriction how-

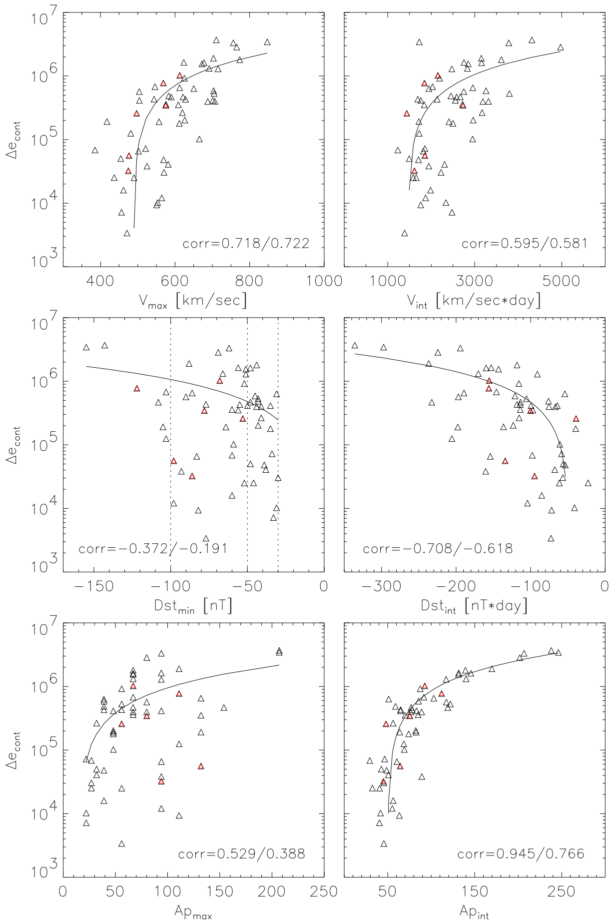

Fig. 2. The left column of panels shows Δe_{cont} versus the maximum values of (t.t.b) V_{sw}, Dst, and Ap and the right column of panels shows Δe_{cont} versus the integrated values of the same parameters. The solid lines represent the best linear fits. The two values of corr in each panel are the correlation coefficients with Δe_{cont} and $\log(\Delta e_{cont})$, respectively.

ever, that $t_{stop} - t_{start}$ must be at least 3.5 days. This restriction was applied to guarantee that for certain CME induced events, not the first e_{cont}-peak was selected which often occurs when the IMF_z turns northward (see e.g. [24]) but the one associated with the slow increase we intend to investigate here. There are however only 6 events in our list for which this restriction applies. These events are plotted as red triangles in figure 2. The definition of the start time may seem a little vague. However, it comes out that changes of t_{start} by a few hours, which is also the temporal resolution of t_{stop} given by the period of the orbit, do not alter the results of the presented analysis. The average length of the period t_{start}, t_{stop} for the selected events is ≈ 5 days.

In order to quantify the electron flux increases we calculated for each event Δe_{cont}, which is the difference between e_{cont} measured at time t_{stop} and the minimum e_{cont} measured between t_{start} and t_{stop}. Then we computed the correlation between Δe_{cont} and solar wind/geomagnetic parameters either by using the maximum values of the parameters measured between t_{start} and t_{stop} or by using the integrated values between t_{start} and t_{stop}. In figure 2 the results for selected parameters are shown. The left column of panels shows Δe_{cont} versus the maximum values of (t.t.b) V_{sw}, Dst, and Ap and the right column of panels shows Δe_{cont} versus the integrated values of the same parameters. The solid lines show the best linear fits and the two values of corr, marked in each panel represent the correlation coefficients with Δe_{cont} and $\log(\Delta e_{cont})$, respectively.

The results for V_{sw} and Dst confirm the earlier findings with data from GEO, that the post-event fluxes tend to scale with the maximum solar wind velocity [25] and that there is only a bad correlation with minimum Dst [13]. The correlation with Dst is significantly improved when using $Dst_{\rm int}$ instead of $Dst_{\rm min}$. However, the best correlation is found with the integrated value of Ap, $Ap_{\rm int}$. We computed the correlation also for other parameters not shown here, like the solar wind dynamic pressure, ϵ, E_y, and $ASY - H$, but non of them correlates with Δe_{cont} as good as $Ap_{\rm int}$ does.

3 Discussion and conclusion

The good correlation between Δe_{cont} and $Ap_{\rm int}$ suggest that the mechanism producing the relativistic electrons in the outer belt is related with substorm activity. The fact that there are several events with a relatively large maximum Ap value but only small electron enhancement (see left Ap-panel in figure 2) indicates that not primarily large substorms, but rather enhanced substorm activity over an extended period is needed to produce the high energy electrons.

Substorms are often associated with injections of electrons with energies of up to several hundred keV into the inner magnetosphere as is regularly observed at geosynchronous orbit [26]. And it was suggested that these injections are the first step in the chain of processes which result in the occurrence of the relativistic electron enhancements [14]. Our data does not allow to judge whether the injections are a necessary condition for an electron enhancement to happen but they strongly suggest that it is not a sufficient condition. A detailed examination of the high-$Ap_{\rm max}$/low-$Ap_{\rm int}$-events shows that large Ap-values, potentially associated with energetic electron injections, occur at the beginning of the events. But if the substorm activity ceases after a day or so, then the increase in the relativistic electrons is small. On the other hand the correlation gets significantly worse if we compute $Ap_{\rm int}$ only over the increase phase of the events showing that the substorm activity during the initial phase is important as well.

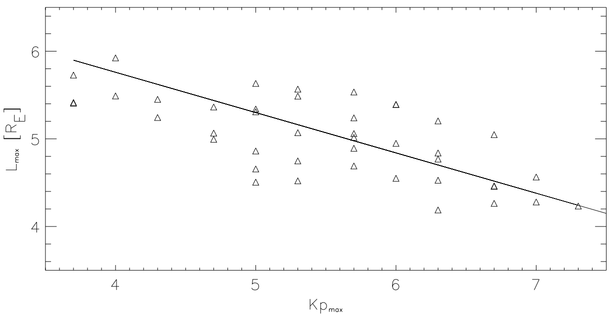

Fig. 3. Post-event peak position of radial REM count rate distribution, $L_{\rm max}$ versus $Kp_{\rm max}$. The value of the slope of the bold line is the one used by *Carpenter and Anderson* [27] to model the the position of the plasmapause as function of $Kp_{\rm max}$.

At this point in the process the convection electric field associated with the build up of the storm main phase could be influential, since it could carry the energetic particles deeper into the trapping region. And it could be expected that the stronger the storm the deeper in the electrons could be taken. Indeed it was shown [28] that there is a relation between the storm magnitude measured with Dst and the L-value, $L_{\rm max}$ at which the post-event electron fluxes peak. The larger the storm, at the lower L-values the peak position is. This relation is also seen for our events with $L_{\rm max} \approx 5.5$ $\rm R_E$ for storms with $Dst_{\rm min} > -50$ nT, $L_{\rm max} \approx 5.0$ $\rm R_E$ for storms with $-100 < Dst_{\rm min} < -50$ nT, and $L_{\rm max} \approx 4.5$ $\rm R_E$ for storms with $Dst_{\rm min} < -100$ nT. However, an alternative explanation for this dependence is lined out below.

Interactions of electrons with different kinds of waves can lead to acceleration of the involved particles. And since during storms and substorms wave activity is high this class of mechanism can be expected to be especially efficient at the geomagnetic conditions shown here to be promotive for relativistic electron enhancements. *Horne and Thorne* [29] have discussed various wave modes which via resonant wave-particle interaction are able to accelerate energetic electrons to the MeV-range. More detailed scenarios were worked out including ULF-waves in combination with pitch-angle scattering [30] and convection [31], and whistler mode waves [32, 33]. As *Horne and Thorne* pointed out the most effective whistler modes are generated within the plasmasphere. Thus if these waves are dominantly involved in the acceleration process it can be expected that the acceleration region will depend on the plasmapause location.

Peaks in the radial distribution of the phase space density, $f(M, K, L)$ (M, K: adiabatic invariants) are indicative for a local heating process. Thus an analysis of the phase space density distribution allows to identify the acceleration region. Using data from the HIST instrument aboard Polar it was demonstrated [31,32] that for selected cases the phase space density distribution of the high energy electrons has a peak typically between 4 and 6 $\rm R_E$ but it was also pointed out that the uncertainties are large due to the inaccuracies of the magnetic field models involved in the computation of f, especially during geomagnetic active periods.

In order to compute an L-distribution of phase space density at fixed M and K, one needs to know the electron energy spectra over a large energy range, which can not be obtained from REM data with the required accuracy. Instead we use count rate profiles and determine the L-value, $L_{\max}$ at which the post-event radial count rate profiles peak. In figure 3, $L_{\max}$ is plotted versus $Kp_{\max}$, which is the maximum Kp-value measured the day before $L_{\max}$ was determined. The solid line is calculated with $L_{\max} = 7.6 - 0.46 \cdot Kp_{\max}$ $\mathrm{R_E}$. The value of the slope is the one used by *Carpenter and Anderson* [8] to model the position of the plasmapause as function of $Kp_{\max}$ and obviously fits very well the $Kp_{\max}$-dependence of $L_{\max}$. Since we are not using phase space density this result is not conclusive, but however indicative for a source region varying in location with the plasmapause. If this result can be confirmed by an investigation of phase space density profiles it would be very supportive for models which predict this dependence [33].

In this paper we did not make a difference between CME and CIR induced events. Since the investigated period from 1995 to 1998 is around solar-minimum most of our events are associated with CIRs. However, the few CME-events shown in figure 2 as red points suggest, that there is no principal difference in the processes responsible for the slow electron increases in the two types of events . The Δe_{cont} of both types of events seem to have a similar Ap_{int}-dependence.

Considering the build-up of the ring-current, which is the main manifestation of a magnetic storm, we note that the processes leading to this build-up (injection, convection [36]) do not necessarily result in the production of relativistic electrons. Through the Dst-effect a strong ring-current rather has a negative effect on the trapped electrons and finally leads to losses. The observations suggest that it needs an additional process or processes, of which wave-particle interactions are good candidates, which are related with substorm activity to act for an elongated period to produce the relativistic electrons.

Acknowledgements

This work was supported by ESA's Technology Research Program, ESA/TOS-EMA, Space Environments and Effects Major Axis, contract 11108/94/NL/JG(SC).

References

[1] McIlwain, C.E., Processes acting upon outer zone electrons, *Geophysical Monograph* **97** (1996) 15.

[2] Roederer, J.G., *Dynamics of Geomagnetically Trapped Radiation*, 166 pp., Springer-Verlag, Berlin (1970)

[3] Schulz, M. and Lanzerotti, J.L., *Particle Diffusion in Radiation Belts*, 215 pp., Springer-Verlag, Berlin (1974)

[4] Lyons, L.R. and Thorne, R.M., Equilibrium structure of radiation belt electrons, *J. Geophys. Res.* **78** (1973) 2142.

[5] Selesnick, R.S., Blake, J.B., Kolasinski, W.A., and Fritz, T.A., A quiescent state of 3 to 8 MeV radiation belt electrons, *Geophys. Res. Lett.* **24** (1997) 1343.

[6] Baker, D.N., Blake, J.B., Callis, L.B., Belian, R.D., and Cayton, T.E., Relativistic electrons near geostationary orbit: evidence for internal magnetospheric acceleration, *Geophys. Res. Lett.* **16** (1989) 559.

[7] Frank, L.A., Inward radial diffusion of electrons of greater than 1 million electron volt in the outer radiation zone, *J. Geophys. Res.* **70** (1965) 3533.

[8] Li, X., Baker, D.N., Temerin, M., Cayton, T.E., Reeves, E.G.D., Christensen, R.A., Blake, J.B., Looper, M.D., Nakamura, R., and Kanekal, S.G., Multisatellite observations of the outer zone electron variation during Nov. 3-4, 1993, magnetic storm, *J. Geophys. Res.* **102** (1997) 14123.

[9] Blake, J.B., Baker, D.N., Turner, N., Ogilvie, K.W., and Lepping, R.P., Correlation of changes in the outer-zone relativistic-electron population with upstream solar wind and magnetic field measurements, *Geophys. Res. Lett.* **24** (1997) 927.

[10] Iles, R.H.A., Fazakerley, A.N., Johnstone, A.D., and Bühler, P., Relativistic electron flux enhancements in the outer radiation belt, *Geophys. Res. Lett.* submitted (2000).

[11] Desorgher, L., Bühler, P., Zehnder, A., Daly, E., and Adams, L., Outer radiation belt variations during 1995, *Adv. Space Res.* **22** (1998) 83.

[12] Baker, D.N., Kanekal, S.G., Pulkinnen, T.I., Blake, J.B., Equinoctial and solsticial averages of magnetospheric relativistic electrons: A strong semiannual modulation, *Geophys. Res. Lett.* **26** (1999) 3193.

[13] Reeves, G.D., Relativistic electrons and magnetic storms: 1992-1995, *Geophys. Res. Lett.* **25** (1998) 1817.

[14] Baker, D.N., Li, X., Blake, J.B., and Kanekal, S., Strong electron acceleration in the earth's magnetosphere, *Adv. Space Res* **21** (1998) 609.

[15] Bühler, P., Ljungfelt, S., Mchedlishvili, M., Schlumpf, N., Zehnder, A., Adams, L., Daly, E., and Nickson, R., Radiation Environment Monitor *Nuclear Instruments and methods A* **386** (1996) 825.

[16] Lepping, R.P. et al., The Wind magnetic field investigation, *Space. Scie. Rev.* **71** (1995) 207.

[17] Ogilvie, K.W. et al., SWE, a comprehensive plasma instrument for the Wind spacecraft, *Space. Scie. Rev.* **71** (1995) 55.

[18] GEOMAG, NOAA National Data Centers, NGDC, High Resolution Geomagnetic Data, http://www.ngdc.noaa.gov/stp/GEOMAG/geomag1.html.

[19] Dessler, A.J. and Karplus, R., Some effects of diamagnetic ring currents on Van Allen radiation, *J. Geophys. Res.* **66** (1966) 2289.

[20] Kim, H.-J. and Chan, A.A., Fully adiabatic changes in storm time relativistic electron fluxes, *J. Geophys. Res.* **102** (1997) 22107.

[21] Nakamura, R., Kamei, K., Kamide, Y., Baker, D.N., Blake, J.B., and Looper, M., SAMPEX observations of storm-associated electron flux variations in the outer radiation belt, *J. Geophys. Res.* **103** (1998) 26261.

[22] Desorgher, L., Bühler, P., Zehnder, A. and Flückiger, E, Simulation of the outer electron belt dropout during the March 26, 1995 magnetic storm, *J. Geophys. Res.* accepted (2000).

[23] Desorgher, L., Flückiger, E, Bühler, P., and Zehnder, A., Modelling of the outer electron belt flux dropout and losses during magnetic storm main phase, *Adv. Space Res.* **26** (2000) 167.

[24] Bühler, P., Johnstone, A., Desorgher, L., Zehnder, A., Daly, E., and Adams, L., The outer radiation belt during the 10 January, 1997 CME event, *Geophys. Res. Lett.* **25** (1998) 2983.

[25] Paulikas, G.A. and Blake, J.B., Effects of the solar wind on magnetospheric dynamics: energetic electrons at the synchronous orbit, *Geophysical Monograph* **21** (1979) 181.

[26] Birn, J., Thomsen, M.F., Borovsky, J.E., Reeves, G.D., McComas, D.J., Belian, R.D., and Hess, M., Substorm electron injections: Geosynchronous observations and test particle simulations, *J. geophys. Res.* **103** (1998) 9235.

[27] Carpenter, D. and Anderson, R., An ISEE/whistler model of the equatorial electron density in the magnetosphere, *J. Geophys. Res.* **97** (1992) 1097.

[28] Tverskaya, L.V., The latitude position dependence of the relativistic electron maximum as a function of *Dst*, *Adv. Space Res.* **18** (1995) 135.

[29] Horne, R.B. and Thorne, R.M., Potential waves for relativistic electron scattering and stochastic acceleration during magnetic storms, *Geophys. Res. Lett.* **25** (1998) 3011.

[30] Liu, W.W., Rostoker, G., and Baker, D.N., Internal acceleration of relativistic electrons by large-amplitude ULF pulsations, *J. Geophys. Res.* **104** (1999) 17391.

[31] Elkington, S.R., Hudson, M.K., and Chan, A.A., Acceleration of relativistic electrons via drift-resonant interaction with toroidal-mode Pc-5 ULF oscillations, *Geophys. Res. Lett.* **26** (1999) 3273.

[32] Summers, D., Ma, C.-y., A model for generating relativistic electrons in the Earth's inner magnetosphere based on gyroresonant wave-particle interactions, *J. Geophys. Res.* **105** (2000) 2625.

[33] Boscher, D., Bourdarie, S., Thorne, R., and Abel, B., Influence of the wave characteristics on the electron radiation belt distribution, *Adv. Space Res.* **26** (2000) 163.

[34] Selesnick, R.S. and Blake, J.B., Dynamics of the outer belt, *Geophys. Res. Lett.* **24** (1997) 1347.
[35] Selesnick, R.S. and Blake, J.B., On the source location of radiation belt relativistic electrons, *J. Geophys. Res.* **105** (2000) 2607.
[36] Kamide, Y., Baumjohann, W., Daglis, I.A., et al., Current understanding of magnetic storms: Storm-substorm relationship, *J. Geophys. Res* **103** (1998) 17705.